Sensors and Actuators B 267 (2018) 328–335

Contents lists available at ScienceDirect

Sensors and Actuators B: Chemical

journal homepage: www.elsevier.com/locate/snb

Enzymatically driven formation of palindromic DNA-Au nanoparticles for snowball assembly and colorimetric biosensing

Yawei Wang, Jingxing Guo, Yuehua Guo, Xiaobo Zhang, Huangxian Ju *

State Key Laboratory of Analytical Chemistry for Life Science, School of Chemistry and Chemical Engineering, Nanjing University, Nanjing 210023, PR China

ARTICLE INFO

Article history:
Received 18 January 2018
Received in revised form 7 April 2018
Accepted 11 April 2018

Keywords:
Snowball assembly
Enzymatically driven recycling
Colorimetric biosensing
Scanometric assay
DNA analysis
Protein detection

ABSTRACT

A strategy for enzymatically driven formation of palindromic DNA-Au nanoparticles (AuNPs) was designed via specific recycling recognition and release of target DNA to/from hairpin DNA functionalized AuNPs (DNA-AuNPs), which led to the snowball assembly of palindromic DNA-AuNPs at single temperature. The assembly was demonstrated with UV–vis spectra, TEM images, dynamic light scattering and PAGE analyses, and could be monitored by substantial red shift of the adsorption peak and the colour change of DNA-AuNPs from red to pink and ultimately slight purple, leading to a convenient method for colorimetric detection of target DNA. By combining with AuNPs-catalyzed silver enhancement, sensitive and selective scanometric assay was further achieved. This strategy could be extended to a wide range of analytes by coupling with other strategies releasing tag DNA from a DNA duplex upon the recognition of target analyte for enzymatically driven formation and snowball assembly of palindromic DNA-nanoparticles. As a proof-of-concept, the extended methods for thrombin detection showed excellent biosensing performance, indicating universal applicability of the proposed strategy for colorimetric biosensing of both DNA and proteins.

1. Introduction

Since the pioneer works were reported by Mirkin and Alivisatos [1,2], DNA functionalized gold nanoparticles (DNA-AuNPs) have become powerful tools for specific biosensing and bioimaging because of their exceptional programmable capability and outstanding chemical and physical properties [3,4]. These programmable nanoscale materials can be assembled into well-defined architectures with accurate spacings, directional orientations and stereo-relationships [3,5]. The assembly of DNA-AuNPs is not only associated with themselves (such as the core and surface chemistry), but also with the external stimuli, such as temperature and salt concentration [5–8]. Furthermore, DNA-AuNPs can be driven into predictable architectures by electrolyte [8], temperature [9,10], and DNA nanotechnology [9–13], which generally needs a linker DNA or template DNA, such as DNA origami or DNA nanotube, to bridge the DNA-AuNPs for facilitating the assembly [11,13]. As a structure used in DNA nanotechnology, the palindromic DNA sequence provides a convenient way to control the assembly with a thermal annealing process in the help of assistant DNA [9,10]. Therefore, this work designed a novel strategy for enzymatically driven formation of palindromic DNA-AuNPs via specific recycling recognition and release of target DNA to/from hairpin DNA functionalized AuNPs (DNA-AuNPs) and snowball assembly of form palindromic DNA-AuNPs for target DNA analysis.

Due to the simplicity, low cost and time-saving, AuNPs-based colorimetric sensors have been attracting more considerable interests and been widely used to detect metal ions [14–16], nucleic acids [17–23], small organic molecules [23–26] and proteins [23,27,28]. These colorimetric sensors can be classified into two detection manners, crosslinking assembly and non-crosslinking aggregation. The former manner is performed using cross-linker DNA or target DNA to form duplex DNA-AuNPs assemblies [14–21,24]. The non-crosslinking aggregation is usually induced with salts to regulate the stability of AuNPs or aptamer functionalized AuNPs for recognition of the substrate [22,25–28]. The cross-linking mode exhibits more rapid colour change in the presence of a small number of cross-linker DNA, which is favourable for detection of target analytes with higher sensitivity [29]. However, this mode needs an annealing step [14] or two kinds of DNA modified AuNPs to realize the hybridization assembly [15,30]. The multiplex-step procedure hinders its practical onsite application. Therefore it is critically important to develop one more simple colorimetric sensing strategy for rapid detection of targets.

Here, the enzymatically driven formation and following snowball assembly of palindromic DNA-AuNPs could be achieved at single step and temperature due to the cyclic hybridization of target DNA with hairpin DNA co-immobilized on AuNPs to form a double-

* Corresponding author.
E-mail address: hxju@nju.edu.cn (H. Ju).

https://doi.org/10.1016/j.snb.2018.04.062
0925-4005/

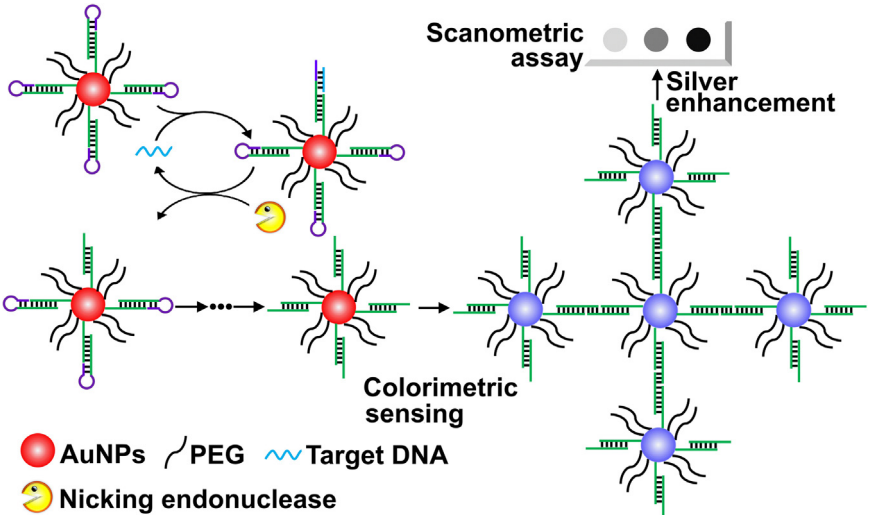

Scheme 1. Enzymatically driven formation and snowball assembly of palindromic DNA-AuNP conjugates for colorimetric sensing and visual detection of target DNA in help of silver enhancement.

helix structure with a recognition site for nicking endonuclease, Nt.BbvCI [31–33], which led to the release of target DNA from the AuNPs (Scheme 1). Interestingly, the short sequence of palindromic DNA and large steric hindrance made their hybridization on the same AuNP impossible, and the natural hybridization of formed palindromic DNA on different AuNPs changed the aggregation state of AuNPs and thus the solution colour, which led to a colorimetric method for detection of target DNA. By combining with AuNPs-catalyzed silver enhancement [30,34,35], a sensitive and selective scanometric assay for target DNA was further proposed. Furthermore, this strategy possessed universal applicability for both DNA and protein analyses. The latter could be achieved using a DNA duplex, which contained a tag DNA and an aptamer sequence for the target protein, to recognize the protein for release of tag DNA as a substitute of target DNA (Scheme S1). To our best knowledge, this is the first example to use enzyme as a regulator to drive the formation and snowball assembly of palindromic DNA-AuNPs for colorimetric sensing. Due to the simplicity, convenience, low cost and rapidity, this strategy is capable of point-of-care diagnosis.

2. Experimental

2.1. Materials and reagents

Gold (III) chloride trihydrate ($HAuCl_4$), tris (2-carboxyethyl) phosphine hydrochloride solution (TCEP, 0.5 M, pH 7.0), tris (hydroxymethyl) aminomethane, (3-aminopropyl) triethoxysilane (APTES, ≥99%), thrombin from human plasma, hemoglobin (Hb) from bovine blood, albumin (ALB) from chicken egg white, casein (CS) from bovine milk, silver enhancement solutions A and B were purchased from Sigma-Aldrich Inc. (USA). Trisodium citrate dihydrate was obtained from Nanjing Chemical Reagent Co., Ltd. (Nanjing, China). Thiol PEG 2000 (PEG) was obtained from Jenkem Technology Ltd. (Beijing, China). Nt.BbvCI as well as 10 × NEB buffer (pH 7.9 at 25 °C) was obtained from New England BioLabs Inc. (USA). Thrombin aptamer (TBA) and tag DNA were dissolved in Tris-HCl buffer 1 (10 mM, pH 7.9) containing 50 mM KCl and 10 mM $MgCl_2$. Tris-HCl buffer 2 (10 mM, pH 7.9) containing 50 mM NaCl and 10 mM $MgCl_2$ was used to prepare the stock solutions of other oligonucleotides. Thrombin solution was prepared in Tris-HCl buffer 3 (20 mM, pH 7.4) containing 140 mM NaCl, 5 mM KCl, 1 mM $CaCl_2$ and 1 mM $MgCl_2$. NEB buffer (1 ×) was used for colorimetric sensing and scanometric assay. All other reagents were of analytical grade and used without further purification. All aqueous solutions were prepared using ultrapure water (≥18 MΩ, Milli-Q, Millipore). Oligonucleotides were obtained from Sangon Biotechnology Inc. (Shanghai, China), and the oligonucleotide sequences were listed in Table S1.

2.2. Apparatus

The UV–vis-NIR absorption spectra were obtained with a UV-3600 UV–vis-NIR spectrophotometer (Shimadzu Co., Kyoto, Japan). The images of the silver spot on indium tin oxide (ITO) glass slides were scanned with HP scanner. Dynamic light scattering (DLS) and Zeta potential analyses were performed on a 90 Plus/BI-MAS equipment (Brook haven, USA). The static water contact angles were measured with a contact-angle system (OCA30, Dataphysics Instruments GmbH, Germany) using droplets of 1 μL of ultrapure water at room temperature. The transmission electron microscopic (TEM) images were obtained on a JEM-2100 transmission electron microscope (JEOL Ltd., Japan). The polyacrylamide gel electrophoresis was performed on the Mini-PROTEAN Tetra System and imaged on Bio-rad ChemDoc XRS (Bio-Rad, USA).

2.3. Preparation of hairpin DNA-AuNPs

AuNPs around 40 nm were synthesized according to previous work [15]. In brief, 0.45 mL of 38.8 mM trisodium citrate dihydrate was quickly added into 50 mL boiling solution of 0.3 mM $HAuCl_4$ under vigirous stirring. After the solution became red, it was heated for another 30 min and slowly cooled to the room temperature. The resulting AuNPs were washed thrice by centrifugation under 9500 rpm for 15 min and resuspended in 35 mL ultrapure water.

Hairpin DNA-AuNPs were conducted according to literature procedures with small modifications [9,36,37]. Firstly, 3′-thiol oligonucleotide (cDNA1) was activated with TCEP at a mole ratio of TCEP to cDNA1 of 198: 1 under vigorous shaking for 2 h at room temperature. 47 μL of the activated cDNA1 was mixed with PEG at the mole ratio of 1:1, and added into 7 mL of AuNPs to incubate at room temperature overnight. Afterwards, 72 μL of 1% wt tween-20 and 72 μL of 1 M Tris-HCl (pH 7.9) were added into the mixture, and 3 M NaCl containing 0.01% wt tween-20 was stepwise added into the solution at 1–2 h intervals to a final NaCl concentration of 0.5 M. The mixture was then allowed to incubate at room temperature overnight with shaking. After excess cDNA1 and PEG were

removed from the solution by thrice centrifugation under 9500 rpm for 15 min, the product was resuspended in 7 mL Tris-HCl buffer (10 mM, pH 7.9) containing 50 mM NaCl and 10 mM $MgCl_2$. Subsequently, the obtained cDNA1-AuNP conjugates were incubated with hairpin DNA (equivalent to cDNA1) for 8–10 h at room temperature with shaking, and the excess hairpin DNA was washed for three rounds by centrifugation under 9500 rpm for 15 min. Finally, the resulting hairpin DNA-AuNPs were dispersed in 10 mL of 1 × NEB buffer and stocked at 4 °C for further experiments.

2.4. Preparation of APTES-modified indium tin oxide (ITO) glass slides

After the ITO glass slides were cleaned with ultrapure water, acetone, ethanol in turn under ultrasonic for 15 min, they were immersed into basic piranha solution (the mixture of 60 mL H_2O, 22.5 mL H_2O_2, and 22.5 mL $NH_3 \cdot H_2O$) at 80 °C for 1 h, washed thrice with ultrapure water and dried under a stream of nitrogen. The glass slides were then modified with 10% APTES in toluene for 3 h at room temperature, washed in turn with toluene, acetone, ultrapure water, and dried under a stream of nitrogen to obtain the APTES-modified ITO glass slides.

2.5. Measurement procedure

The enzymatically driven formation and snowball assembly of palindromic DNA-AuNPs were performed by mixing 190 μL DNA-AuNPs with 5 μL of 1 U/μL Nt.BbvCI and 5 μL of various concentrations of target DNA. After incubation at 37 °C for 15 min, the reaction solution was characterized with UV–vis absorption spectrometry, DLS and TEM images. The absorbance change at 542 nm with the increasing temperature from 20 °C to 75 °C was also monitored at 0.5 °C intervals with a rate of 0.5 °C min^{-1} to obtain the melting properties of snowball assembled DNA-AuNPs.

For the silver enhancement, 6 μL of reaction solution was transferred onto an APTES-modified ITO glass slide and allowed to dry, and the each spot reacted with 10 μL 1:1 mixture of silver enhancer solutions A and B for 4 min. After washed with ultrapure water and dried under a stream of nitrogen, the glass slides were scanned using a scanner, and the gray-scale intensity of the resulting image was quantified by Adobe Photoshop software to quantify the assembly extent of the DNA-AuNP conjugates. Considering the fact that more silver deposition showed darker spot, which meant lower grey-scale intensity, this work used the relative grey-scale intensity (I) to quantify the signal of the staining spot by subtracting the gray-scale intensity value of the spot from that of the background, which led to higher I value at darker spot.

The protein detection could be performed by mixing 1.5 μM TBA/Tag DNA duplex, 190 μL hairpin DNA-AuNPs, 0.025 U/μL Nt.BbvCI and various concentrations of thrombin to incubate at 37 °C for 60 min. For preparing the TBA/Tag DNA duplex, TBA was mixed with tag DNA and heated at 95 °C for 10 min, followed with slowly cooling to room temperature at a rate of 1 °C min^{-1}.

2.6. Polyacrylamide gel electrophoresis (PAGE) analysis

The 10% native polyacrylamide gel was firstly prepared using 1 × TBE buffer. 7 μL of DNA samples were mixed with 1.5 μL of 6 × loading buffer to obtain the loading samples, which were kept for 3 min before injection into the polyacrylamide hydrogel. After the gel electrophoresis was run at 90 V for 90 min, the gel was stained with GelRed dye, and then photographed with a Molecular Imager Gel Doc XR.

3. Results and discussion

3.1. Synthesis and characterization of AuNPs and hairpin DNA-AuNPs

Considering the fact that the large AuNPs can greatly accelerate the rate of colour change compared to the small AuNPs [15], the AuNPs with a size of 40 nm were chosen as a substrate for colorimetric biosensing. The synthesized AuNPs showed a uniform size with an approximate sphere structure (Fig. S1). The average diameter was about 40 nm. The AuNPs solution showed an absorption peak at 537 nm. After cDNA1/hairpin and PEG were co-immobilized on their surface, the absorption peak red-shifted to 542 nm due to the replacement of citrate by DNA sequence and PEG on the AuNPs (Fig. 1a), which significantly increased the localized refractive index [18], and the hydration diameter (Fig. 1b). The great decrease of Zeta

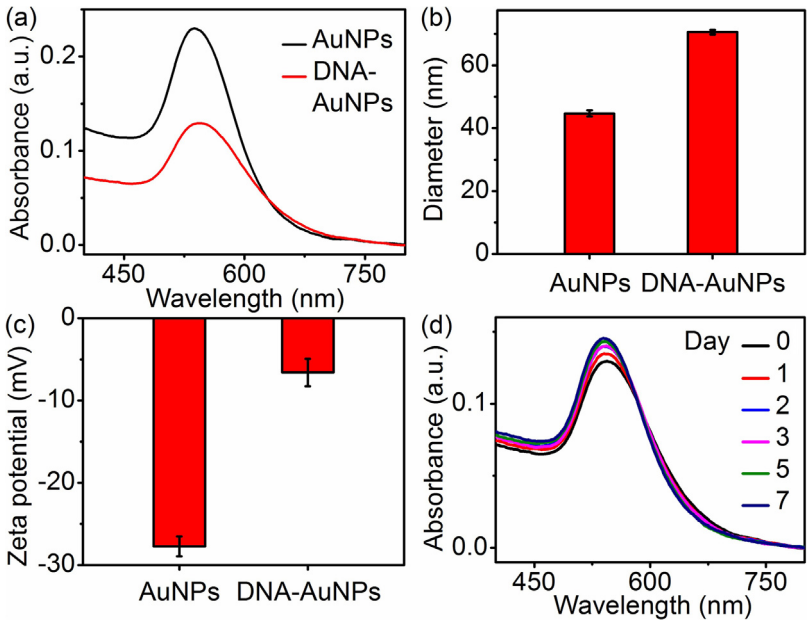

Fig. 1. (a) UV–vis spectra, (b) hydration diameters and (c) Zeta potentials of AuNPs and hairpin DNA-AuNPs, (d) stability of hairpin DNA-AuNPs monitored with UV–vis spectra.

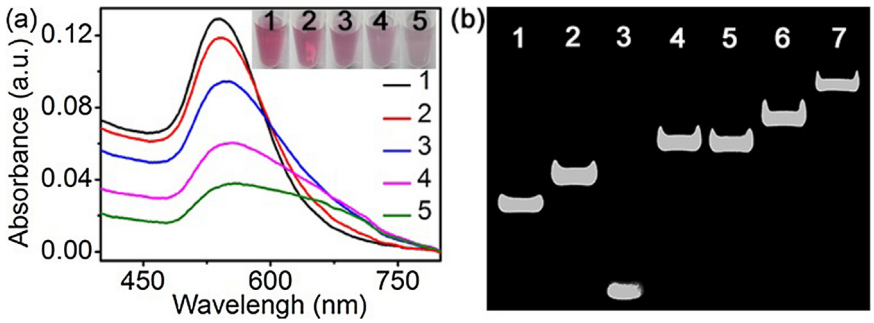

Fig. 2. (a) UV–vis spectra of hairpin DNA-AuNPs solution containing 0.025 U/μL Nt.BbvCI after 20 nM target DNA is added for (1) 0, (2) 15, (3) 30, (4) 45 and (5) 60 min. Inset: Photos of corresponding solutions. (b) PAGE analysis of cDNA2 (1), hairpin DNA (2), target DNA (3), cDNA2 + hairpin DNA (4), hairpin DNA + target DNA (5), cDNA2 + hairpin DNA + target DNA (6), and (6) +Nt.BbvCI (7).

potential demonstrated the replacement of citrate anions by cDNA1 and PEG (Fig. 1c), which led to less negatively charged surface [38–40]. However, the prepared hairpin DNA-AuNPs were stable in one week, which could be monitored from the absorption peak at 542 nm (Fig. 1d).

3.2. Feasibility of snowball assembly and colorimetric sensing

To test the feasibility of the enzymatically driven formation and snowball assembly of palindromic DNA-AuNPs and colorimetric sensing, the colour, UV–vis absorption spectrum and the size of hairpin DNA-AuNPs were monitored upon addition of target DNA in hairpin DNA-AuNPs solution containing Nt.BbvCI. After 20 nM target DNA was added into hairpin DNA-AuNPs solution containing 0.025 U/μL Nt.BbvCI, the colour gradually changed from red to pink, and the characteristic absorption peak at 542 nm red-shifted to 558 nm along with the decrease of peak intensity, while a weak absorption peak occurred at around 700 nm (Fig. 2a), demonstrating the formation of nanoparticle assemblies. The colour change could be observed by naked eye. The formation of nanoparticle assemblies due to the enzymatically driven snowball assembly could be directly characterized with TEM images, which showed the increasing size (Fig. S2). Meanwhile, the snowball assembled DNA-AuNPs showed a very sharp melting transition (Fig. S3), which further confirmed the linkage of palindromic DNA [41].

Polyacrylamide gel electrophoresis (PAGE) analysis was used to verify the hybridization of hairpin DNA with capture DNA, and the recognitions of target DNA to the hairpin DNA and Nt.BbvCI to the cleavage site. To simplify PAGE analysis, capture DNA 2 (cDNA2) with the same sequence as cDNA1 was used to hybridize with hairpin DNA. As shown in Fig. 2b, the monomer DNA band was individually showed in lanes 1, 2 and 3, and two of them could hybridize each other to show a new product DNA band in lanes 4 and 5 compared to their monomer DNA bands. When cDNA2, hairpin DNA and target DNA were mixed, a slower migration band was observed for the triplex product (lane 6). After nicking endonuclease Nt.BbvCI was added into the mixture of DNA (lane 7), a slowest band appeared compared to lane 6, which could be attributed to the formation of dimer product due to the cleavage of target/hairpin DNA structure to trigger the hybridization of the produced palindromic sequences. These results indicated the successful design of enzymatically driven hybridization of DNA sequences, and demonstrated the feasibility of the enzymatically driven formation and snowball assembly of palindromic DNA-nanoparticles.

3.3. Optimization of detection conditions

In order to obtain optimal sensing performance for target DNA, the experimental parameters, such as the reaction time and concentration of Nt.BbvCI, were investigated. The intensity ratio of the adsorption peak around 700 nm to the characteristic absorption peak at 542 nm, A_{700}/A_{542}, was used to assess the effects of the experimental conditions on sensing performance. The ratio value increased quickly at initial stage and changed slowly after 15 min (red line), while the background signal did not change significantly (black line) (Fig. 3a), which meant that the reaction time of 15 min could give the better signal-to-noise ratio for target analysis. The value of A_{700}/A_{542} also increased with an increasing concentration of Nt.BbvCI *Nt.B*bvCI and attained a relatively stable plateau at 0.025 U/μL Nt.BbvCI (red line), while background signal did not obviously change (black line) (Fig. 3b), indicating that the optimum concentration of Nt.BbvCI was 0.025 U/μL. The sensing performance also depended on the pH and temperature of detection solution, which affected the activity of Nt.BbvCI and assembly rate. The optimal pH value and temperature were demonstrated to be 7.9 and 37 °C (Fig. 3c–d).

3.4. Colorimetric sensing and scanometric assay of DNA

After target DNA was introduced into the solution containing DNA-AuNPs and Nt.BbvCI, the snowball assembly led to the change of optical properties of DNA-AuNPs (Fig. 4a). With the increasing concentration of target DNA, the adsorption peak of DNA-AuNPs at 542 nm red-shifted to longer wavelength, and the intensity also decreased gradually, while the intensity of the weak absorption peak at around 700 nm increased due to the formation of assembled aggregates, which was similar to the previous report [15]. The intensity ratio of the adsorption peak around 700 nm to the plasmonic peak at 542 nm, A_{700}/A_{542}, could be used to quantitatively analyze the concentration of target DNA (Fig. 4b), which showed a dynamically increasing response in the concentration range of 10 nM to 1000 nM, and a linear relationship ranging from 10 to 70 nM with a detection limit of 9.2 nM. The colour of detection solution changing from red to pink and ultimately slight purple could also be used to estimate the target concentration by naked eye (Fig. 4c).

The formation of assembled aggregates was further demonstrated through the measurement of hydration diameter, which showed the dynamic increase similar to that of A_{700}/A_{542} as the concentration of target DNA increased (Fig. S4). The TEM images also confirmed the formation of assembled aggregates (Fig. S5). Thus the proposed enzymatically driven snowball assembly of DNA-AuNP conjugates was a successful architecture.

The ability of the colorimetric sensing to distinguish the target DNA from the mismatched sequences was necessary for the point-of-care diagnosis. After the detection solution containing DNA-AuNPs and 0.025 U/μL Nt.BbvCI was individually incubated with 50 nM target DNA, and 10-folds single-base mismatched DNA,

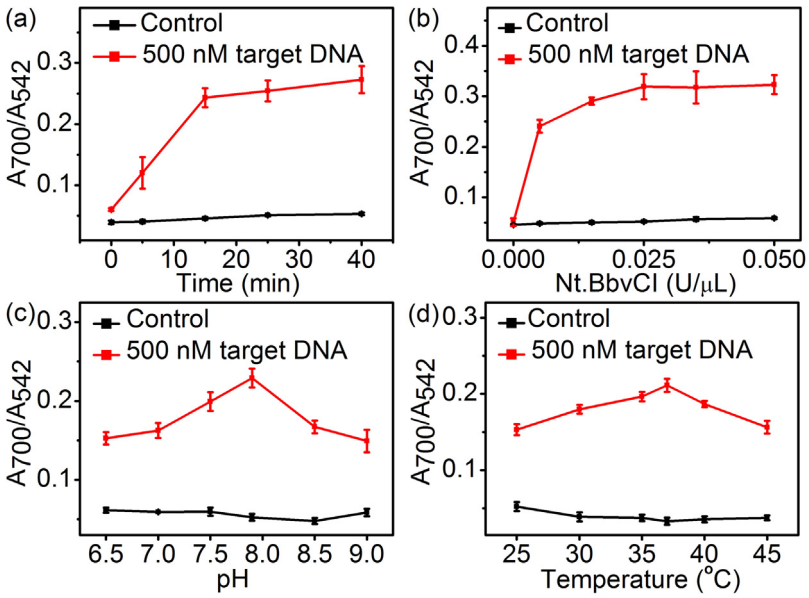

Fig. 3. Plots of A_{700}/A_{542} vs (a) reaction time, (b) Nt.BbvCI concentration, (c) pH value and (d) reaction temperature in the absence (control) and presence of 500 nM target DNA.

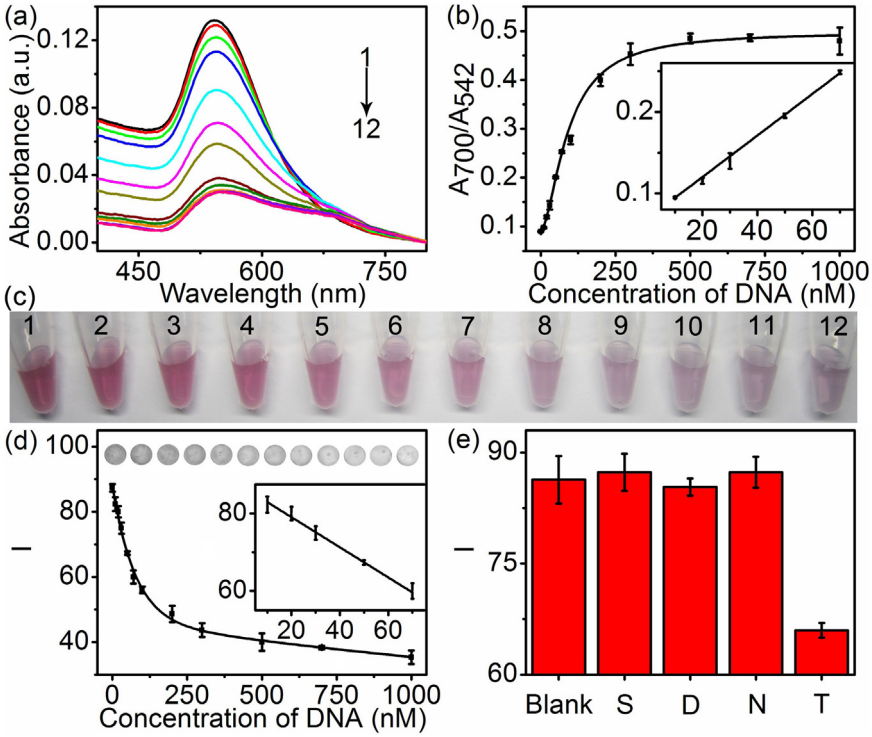

Fig. 4. (a) UV–vis spectra of detection solution containing hairpin DNA-AuNPs and 0.025 U/μL Nt.BbvCI upon addition of 0, 10, 20, 30, 50, 70, 100, 200, 300, 500, 700 and 1000 nM target DNA (from 1 to 12, respectively) for 15 min. (b) Dependence of A_{700}/A_{542} on target DNA concentration. Inset: Calibration curve. (c) Images of corresponding samples in (a). (d) Plot of relative grey-scale intensity vs concentration of target DNA and scanometric images of corresponding spots at 0, 10, 20, 30, 50, 70, 100, 200, 300, 500, 700 and 1000 nM (from left to right). Inset: Calibration curve. (e) Selectivity of scanometric assay for 0 (blank), 50 nM target DNA (T), and 500 nM single-base mismatched DNA (S), double-bases mismatched DNA (D) and noncomplementary DNA (N).

double-bases mismatched DNA and noncomplementary DNA, only target DNA showed the statistically significant response (Fig. S6), and all other DNA sequences did not produce obvious changes in the absorption spectrum compared to the blank. This result indicated the excellent selectivity of this designed colorimetric sensing strategy. The high specificity was attributed to the conformational constraint of the stem-loop structure of the hairpin in DNA-AuNPs for thermodynamically unfavourable binding of the mismatched DNA to the loop due to the existence of stem [30]. Thus the colorimetric sensing strategy was a reliable method for DNA detection. Besides, benefiting from snowball assembly of palindromic DNA-AuNPs and the enzymatically driven recycling strategy, the proposed colorimetric sensing method showed relatively short assay time with simpler operation steps compared with previous methods for DNA detection (Table S2).

To improve the sensing performance of the visualization method, the snowball assembly was combined with AuNP-catalyzed silver signal amplification for scanometric DNA array,

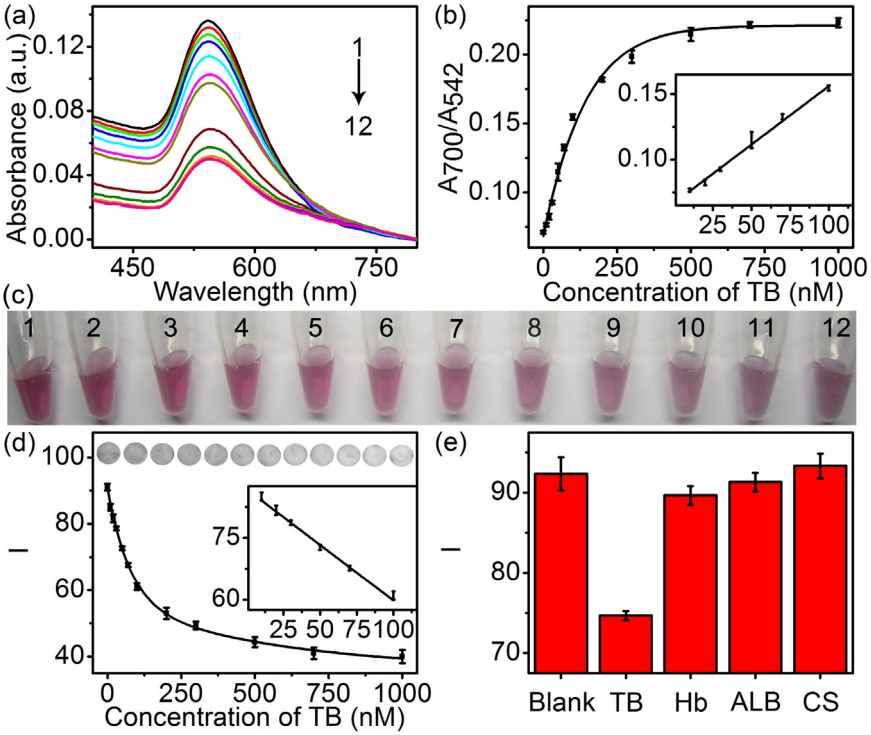

Fig. 5. (a) UV–vis spectra of detection solution containing hairpin DNA-AuNPs, 0.025 U/μL Nt.BbvCI and 1.5 μM TBA/Tag DNA upon addition of 0, 10, 20, 30, 50, 70, 100, 200, 300, 500, 700 and 1000 nM thrombin (from 1 to 12, respectively) to react for 60 min. (b) Dependence of A_{700}/A_{542} on thrombin concentration. Inset: Calibration curve. (c) Images of corresponding samples in (a). (d) Plot of relative grey-scale intensity vs concentration of thrombin and scanometric images of corresponding spots at 0, 10, 20, 30, 50, 70, 100, 200, 300, 500, 700 and 1000 nM (from left to right). Inset: Calibration curve. (e) Selectivity of scanometric assay for blank, 50 nM TB, and 500 nM Hb, ALB and CS.

which can be performed with a conventional flatbed scanner as a reader to accomplish high-throughput DNA detection [42]. After the snowball assembly, the detection solution was transferred onto an APTES-modified ITO glass slide, which led to the binding of free DNA-AuNP conjugates and the assembled aggregates to ITO glass slide via the interaction of primary amine group with Au atom. The modification of APTES on ITO glass slide was characterized with contact angle measurements (Fig. S7), which showed a contact angle change from 69° to 37° due to the presence of the amino group of APTES. The immobilized DNA-AuNP conjugates and aggregates possessed different catalytic activities to the reduction of silver ion by hydroquinone, thus different silver staining spots could be formed on the slide substrate after the mixture of silver enhancer solutions A and B was dropped on these immobilized spots for 4 min. The stronger catalytic activity of dispersed AuNPs produced darker spot on the glass slides than those containing the assembled aggregates [30,34,35]. As expected, the extent of silver enhancement or the relative grey-scale intensity, *I*, was inversely proportional to the concentration of target DNA (Fig. 4d). To avoid the oxidation of hydroquinone by oxygen, whose product usually interferes with the measurement of grey-scale intensity, the silver deposition reaction was carried out within 4 min in multiplex steps. The optimal procedure was performed for 3 times (Fig. S8). After 3-times deposition reactions, the plot of relative grey-scale intensity vs target DNA concentration showed good relationship with a detection limit of 7.7 nM, which was slightly lower than that of the colorimetric sensing. Similarly, the scanometric assay showed the ability to distinguish the target DNA from the mismatched sequences (Fig. 4e).

In order to evaluate the applicability of the DNA detection method in real samples, 50 nM target DNA was spiked into 100-fold diluted human serums to detect the DNA concentration. The colorimetric sensing of target DNA showed a recovery of 98.8% with a RSD of 2.2% ($n = 3$), and the scanometric assay result was also acceptable (Table S3), which indicated that the accuracy and precision of both methods were satisfactory, and this strategy could be used for real sample analysis.

3.5. Protein detection

Using a tag DNA as the substitute of target DNA, this strategy could be conveniently coupled with other strategies releasing the tag DNA to achieve the enzymatically driven formation and snowball assembly of palindromic DNA-nanoparticles, which greatly extended the practicability of this strategy for colorimetric analysis of an extensive range of analyts. As a proof-of-concept, a DNA duplex containing a tag DNA and an aptamer sequence for recognition of target protein was designed. Using thrombin, an important biomolecule in thrombosis, coagulation cascade, hemostasis [43] and pulmonary metastasis [44], as an analyst model, the tag DNA could be released from the DNA duplex upon the recognition of thrombin to its aptamer, TBA (Scheme S1), which led to the red-shift and great intensity decrease of characteristic absorption peak of hairpin DNA-AuNPs due to the snowball assembly of formed palindromic DNA-AuNPs (Fig. S9). Under optimal TBA/Tag DNA concentration of 1.5 μM and reaction time of 60 min (Fig. S10), the colorimetric and scanometric assays of thrombin showed the detection limits of 8.3 and 4.7 nM with the linear range of 10–100 nM, respectively (Fig. 5a–d). These methods also showed acceptable selectivity by comparing their responses to thrombin with those to hemoglobin (Hb), albumin (ALB) and casein (CS) as the potential interferents due to the high specificity and affinity of the aptamer to thrombin (Figs. 5 5e and S11), and could be used for detection of thrombin in real samples with excellent recovery and precision (Table S3), and relatively short assay time and simpler operation steps (Table S2).

4. Conclusion

This work designs a strategy for enzymatically driven formation of palindromic DNA-Au nanoparticles (AuNPs) via specific recycling recognition and release of target DNA to/from hairpin DNA functionalized AuNPs (DNA-AuNPs). The snowball assembly of formed palindromic DNA-AuNPs leads to substantial red shift of the characteristic adsorption peak and the colour change of DNA-AuNPs from red to pink and ultimately slight purple, along with the peak intensity changes, and thus can be monitored for colorimetric sensing of target DNA. By combining with AuNPs catalyzed silver enhancement, the sensitive and selective scanometric assay is achieved. These methods can be extended for protein detection by coupling with other strategies releasing the tag DNA from a DNA duplex upon the recognition of the target analyst for the formation of palindromic DNA-AuNPs, indicating the universal applicability. This strategy is simply and can be rapidly performed at mild environment without any annealing step. It shows excellent biosensing performance, and thus provides an efficient and universal platform for the detection of various analytes in bioassay and clinical diagnosis.

Acknowledgement

We acknowledge the financial support of the National Natural Science Foundation of China (21635005 and 21361162002).

Appendix A. Supplementary data

Supplementary data associated with this article can be found, in the online version, at https://doi.org/10.1016/j.snb.2018.04.062.

References

[1] C.A. Mirkin, R.L. Letsinger, R.C. Mucic, J.J. Storhoff, A DNA-based method for rationally assembling nanoparticles into macroscopic materials, Nature 382 (1996) 607–609.
[2] A.P. Alivisatos, K.P. Johnsson, X. Peng, T.E. Wilson, C.J. Loweth, M.P. Bruchez, et al., Organization of 'nanocrystal molecules' using DNA, Nature 382 (1996) 609–611.
[3] M.R. Jones, N.C. Seeman, C.A. Mirkin, Programmable materials and the nature of the DNA bond, Science 347 (2015) 1–10.
[4] W.B. Rogers, W.M. Shih, V.N. Manoharan, Using DNA to program the self-assembly of colloidal nanoparticles and microparticles, Nat. Rev. Mater. 1 (2016) 16008.
[5] R.J. Macfarlane, B. Lee, M.R. Jones, N. Harris, G.C. Schatz, C.A. Mirkin, Nanoparticle superlattice engineering with DNA, Science 334 (2011) 204–208.
[6] M. Grzelczak, J. Vermant, E.M. Furst, L.M. Liz-Marzan, Directed self-assembly of nanoparticles, ACS Nano 4 (2010) 3591–3605.
[7] W. Liu, J. Halverson, Y. Tian, A.V. Tkachenko, O. Gang, Self-organized architectures from assorted DNA-framed nanoparticles, Nat. Chem. 8 (2016) 867–873.
[8] S. Kewalramani, L.M. Guerrero-Garcia, J.W. Moreau, C.A. Mirkin, M.O. de la Cruz, et al., Electrolyte-mediated assembly of charged nanoparticles, ACS Cent. Sci. 2 (2016) 219–224.
[9] Y. Kim, R.J. Macfarlane, M.R. Jones, C.A. Mirkin, Transmutable nanoparticles with reconfigurable surface ligands, Science 351 (2016) 579–582.
[10] R.J. Macfarlane, R.V. Thaner, K.A. Brown, J. Zhang, B. Lee, S.T. Nguyen, et al., Importance of the DNA bond in programmable nanoparticle crystallization, Proc. Natl. Acad. Sci. U. S. A. 111 (2014) 14995–15000.
[11] W. Liu, M. Tagawa, H.L. Xin, T. Wang, H. Emamy, H. Li, et al., Diamond family of nanoparticle superlattices, Science 351 (2016) 582–586.
[12] D. Yao, T. Song, X. Sun, S. Xiao, F. Huang, H. Liang, Integrating DNA-strand-displacement circuitry with self-assembly of spherical nucleic acids, J. Am. Chem. Soc. 137 (2015) 14107–14113.
[13] K.L. Lau, G.D. Hamblin, H.F. Sleiman, Gold nanoparticle 3D-DNA building blocks: high purity preparation and use for modular access to nanoparticle assemblies, Small 10 (2014) 660–666.
[14] J. Liu, Y. Lu, A colorimetric lead biosensor using DNAzyme-directed assembly of gold nanoparticles, J. Am. Chem. Soc. 125 (2003) 6642–6643.
[15] J. Liu, Y. Lu, Accelerated color change of gold nanoparticles assembled by DNAzymes for simple and fast colorimetric Pb^{2+} detection, J. Am. Chem. Soc. 126 (2004) 12298–12305.
[16] J.H. Lee, Z. Wang, J. Liu, Y. Lu, Highly sensitive and selective colorimetric sensors for uranyl (UO_2^{2+}): development and comparison of labeled and label-free DNAzyme-gold nanoparticle systems, J. Am. Chem. Soc. 130 (2008) 14217–14226.
[17] K. Zagorovsky, W.C. Chan, A plasmonic DNAzyme strategy for point-of-care genetic detection of infectious pathogens, Angew. Chem. Int. Ed. 52 (2013) 3168–3171.
[18] L. Guo, Y. Xu, A.R. Ferhan, G. Chen, D.H. Kim, Oriented gold nanoparticle aggregation for colorimetric sensors with surprisingly high analytical figures of merit, J. Am. Chem. Soc. 135 (2013) 12338–12345.
[19] P. Valentini, P.P. Pompa, A universal polymerase chain reaction developer, Angew. Chem. Int. Ed. 55 (2016) 2157–2160.
[20] Y. Lu, X. Ma, J. Wang, N. Sheng, T. Dong, Q. Song, et al., Visualized detection of single-base difference in multiplexed loop-mediated isothermal amplification amplicons by invasive reaction coupled with oligonucleotide probe-modified gold nanoparticles, Biosens. Bioelectron. 90 (2017) 388–393.
[21] H. Yin, X. Huang, W. Ma, L. Xu, S. Zhu, H. Kuang, et al., Ligation chain reaction based gold nanoparticle assembly for ultrasensitive DNA detection, Biosens. Bioelectron. 52 (2014) 8–12.
[22] K. Sato, K. Hosokawa, M. Maeda, Rapid aggregation of gold nanoparticles induced by non-cross-linking DNA hybridization, J. Am. Chem. Soc. 125 (2003) 8102–8103.
[23] L. Zou, R. Li, M. Zhang, Y. Luo, N. Zhou, J. Wang, et al., A colorimetric sensing platform based upon recognizing hybridization chain reaction products with oligonucleotide modified gold nanoparticles through triplex formation, Nanoscale 9 (2017) 1986–1992.
[24] J. Liu, Y. Lu, Non-base pairing DNA provides a new dimension for controlling aptamer-linked nanoparticles and sensors, J. Am. Chem. Soc. 129 (2007) 8634–8643.
[25] W. Zhao, W. Chiuman, J.C. Lam, S.A. McManus, W. Chen, Y. Cui, et al., DNA aptamer folding on gold nanoparticles: from colloid chemistry to biosensors, J. Am. Chem. Soc. 130 (2008) 3610–3618.
[26] J. Zhang, L. Wang, D. Pan, S. Song, F.Y. Boey, H. Zhang, et al., Visual cocaine detection with gold nanoparticles and rationally engineered aptamer structures, Small 4 (2008) 1196–1200.
[27] C.C. Chang, C.P. Chen, C.Y. Chen, C.W. Lin, DNA base-stacking assay utilizing catalytic hairpin assembly-induced gold nanoparticle aggregation for colorimetric protein sensing, Chem. Commun. 52 (2016) 4167–4170.
[28] X. Wei, Y. Wang, Y. Zhao, Z. Chen, Colorimetric sensor array for protein discrimination based on different DNA chain length-dependent gold nanoparticles aggregation, Biosens. Bioelectron. 97 (2017) 332–337.
[29] G. Wang, Y. Akiyama, S. Shiraishi, N. Kanayama, T. Takarada, M. Maeda, Cross-linking versus non-cross-linking aggregation of gold nanoparticles induced by DNA hybridization: a comparison of the rapidity of solution color change, Bioconjugate Chem. 28 (2017) 270–277.
[30] H. Ji, H. Dong, F. Yan, J. Lei, L. Ding, W. Gao, et al., Visual scanometric detection of DNA through silver enhancement regulated by gold-nanoparticle aggregation with a molecular beacon as the trigger, Chem. Eur. J. 17 (2011) 11344–11349.
[31] K. Ren, J. Wu, Y. Zhang, F. Yan, H. Ju, Proximity hybridization regulated DNA biogate for sensitive electrochemical immunoassay, Anal. Chem. 86 (2014) 7494–7499.
[32] C. Zong, J. Wu, M. Liu, L. Yang, L. Liu, F. Yan, et al., Proximity hybridization-triggered signal switch for homogeneous chemiluminescent bioanalysis, Anal. Chem. 86 (2014) 5573–5578.
[33] C. Zong, J. Wu, M. Liu, F. Yan, H. Ju, High-throughput imaging assay of multiple proteins via target-induced DNA assembly and cleavage, Chem. Sci. 6 (2015) 2602–2607.
[34] Z. Zhang, C. Chen, X. Zhao, A simple and sensitive biosensor based on silver enhancement of aptamer-gold nanoparticle aggregation, Electroanalysis 21 (2009) 1316–1320.
[35] L. Ding, R. Qian, Y. Xue, W. Cheng, H. Ju, In situ scanometric assay of cell surface carbohydrate by glyconanoparticle-aggregation-regulated silver enhancement, Anal. Chem. 82 (2010) 5804–5809.
[36] B. Liu, J. Liu, Methods for preparing DNA-functionalized gold nanoparticles, a key reagent of bioanalytical chemistry, Anal. Methods 9 (2017) 2633–2643.
[37] B. Liu, J. Liu, Freezing directed construction of Bio/Nano interfaces: reagentless conjugation, denser spherical nucleic acids, and better nanoflares, J. Am. Chem. Soc. 139 (2017) 9471–9474.
[38] F. Degliangeli, P. Kshirsagar, V. Brunetti, P.P. Pompa, R. Fiammengo, Absolute and direct MicroRNA quantification using DNA-gold nanoparticle probes, J. Am. Chem. Soc. 136 (2014) 2264–2267.
[39] S.M. Shawky, A.M. Awad, W. Allam, M.H. Alkordi, S.F. El-Khamisy, Gold aggregating gold: a novel nanoparticle biosensor approach for the direct quantification of hepatitis C virus RNA in clinical samples, Biosens. Bioelectron. 92 (2017) 349–356.
[40] M. Schollbach, F. Zhang, F. Roosen-Runge, M.W.A. Skoda, R.M.J. Jacobs, F. Schreiber, Gold nanoparticles decorated with oligo(ethylene glycol) thiols: surface charges and interactions with proteins in solution, J. Colloid Interface Sci. 426 (2014) 31–38.
[41] R. Jin, G. Wu, Z. Li, C.A. Mirkin, G.C. Schatz, What controls the melting properties of DNA-linked gold nanoparticle assemblies? J. Am. Chem. Soc. 125 (2003) 1643–1654.
[42] T.A. Taton, C.A. Mirkin, R.L. Letsinger, Scanometric DNA array detection with nanoparticle probes, Science 289 (2000) 1757–1760.
[43] Y. Niu, M. Chu, P. Xu, S. Meng, Q. Zhou, W. Zhao, et al., An aptasensor based on heparin-mimicking hyperbranched polyester with anti-biofouling interface for sensitive thrombin detection, Biosens. Bioelectron. 101 (2018) 174–180.

[44] M.L. Nierodzik, S. Karpatkin, Thrombin induces tumor growth, metastasis, and angiogenesis: evidence for a thrombin-regulated dormant tumor phenotype, Cancer Cell 10 (2006) 355–362.

Biographies

Yawei Wang is a MS candidate in School of Chemistry and Chemical Engineering, Nanjing University, China. His major research focuses on biosensor.

Jingxing Guo received BS degree from Wuhan University in 2014, and then became a PhD candidate of Nanjing University. His researches focus on developing new analytical methods in surface-enhanced Raman spectroscopy.

Yuehua Guo obtained his PhD degree from School of Chemistry and Chemical Engineering, Nanjing University, China. His major research is DNA analysis.

Xiaobo Zhang is a PhD candidate in School of Chemistry and Chemical Engineering, Nanjing University, China. His major research interest is analytical chemistry for life science.

Huangxian Ju received his BS, MS and PhD degrees from Nanjing University during 1982–1992. He was a postdoc in Montreal University (Canada) from 1996 to 1997 and a guest professor in three universities of Germany and Ireland in 1999–2000. He became an associate and full professor of Nanjing University in 1993 and 1999. He is currently the director of State Key Laboratory of Analytical Chemistry for Life Science. His research interests focus on analytical biochemistry, biosensing and molecular diagnosis. He has published 601 papers in different journals with SCI h-index of 83 (24226 citations) and Google Scholar h-index of 91 with more than 29000 citations.